

Communication

A Beam-Steering Reflectarray Antenna with Arbitrary Linear-Polarization Reconfiguration

Changhao Liu, *Student Member, IEEE*, Songlin Zhou, Fan Yang, *Fellow, IEEE*, Shenheng Xu, *Member, IEEE* and Maokun Li, *Senior Member, IEEE*

Abstract—This work presents a beam-steering reflectarray antenna capable of achieving arbitrary linear polarization (LP) reconfiguration. It utilizes a dual-circular polarization (CP) reconfigurable reflectarray, along with an LP feed horn, to synthesize a LP beam by combining two reflected CP beams in the same direction. The LP states can be dynamically adjusted by tuning the phase constants of the array, which correspondingly modify the wave phases. Experimental validation of the proposed polarization synthesis concept is conducted using a 16×16 dual-CP 1-bit reconfigurable reflectarray operating at 16.8 GHz. This reflectarray generates reconfigurable LP waves with polarization states of LP(0°), LP(45°), LP(90°) and LP(135°). Furthermore, it demonstrates the capability to perform beam scanning, allowing for versatile beam manipulation. The application of this polarization-reconfigurable beam-steering reflectarray is pertinent to beam alignment and polarization synchronization in various wireless communication scenarios, including satellite communication and mobile communication.

Index Terms—Beam steering, electromagnetic surfaces, polarization reconfiguration, reconfigurable intelligent surfaces, reconfigurable reflectarray antennas.

I. INTRODUCTION

IN wireless communications, the demand for signal enhancement necessitates the utilization of high-performance antennas. In particular, the alignment of high-gain beam patterns and the synchronization of polarizations between transmitters (Tx) and receivers (Rx) are vital considerations in antenna design.

Beam-scanning antennas possess the ability to dynamically align beams, which is crucial for point-to-point communications. As a new paradigm of large-aperture antennas, spatial-fed planar reflectarray antennas can generate high-gain beams with significant advantages [1]. Reconfigurable reflectarray antennas (RRAs) employ tunable elements that enable real-time manipulation of the reflected phase on each element, consequently facilitating dynamic steering of beam patterns [2], [3]. The investigation of digital RRAs with 1-bit phase resolution has received significant attention [4]–[10]. Besides, ongoing research efforts also explore 2-bit RRAs and continuously-tuned RRAs, which aim to mitigate the phase quantization loss [11]–[16]. Recent years have witnessed a surge of interest in advanced RRAs with multi-functions [17]. For example, a dual-polarization-multiplexed RRA is proposed

recently, which is capable of independently manipulating the beam patterns for two orthogonal linear polarizations (LPs) [18].

Furthermore, numerous practical communication systems rely on single linear polarizations (LPs). However, as the terminal moves or rotates, the received LP also experiences rotation. Ensuring optimal transmission efficiency necessitates the synchronization of polarizations between Tx and Rx. Traditional methods involve mechanical rotation of either the Tx or Rx to achieve polarization synchronization, but these approaches suffer from the slow polarization switching speed. Real-time polarization synchronization requires dynamic polarization tuning techniques in antenna design.

In particular, polarization reconfigurable surfaces can generate tunable polarizations. By integrating lumped switches on the elements, the scattered polarization states can be dynamically controlled. 1-bit polarization reconfigurable surfaces can generate two switchable polarizations. Various prototypes have demonstrated the transitions among horizontal LP (HLP), vertical LP (VLP), left-hand circular polarization (LCP) and right-hand circular polarization (RCP), such as HLP-VLP [19], LP-CP [20], and LCP-RCP [21]. Additionally, a 2-bit-polarization reconfigurable element has been proposed, enabling the active generation of three polarization states using two independent switches [22]. To achieve dynamic generation of a wider range of polarization states, the temporal-modulation technique is employed for arbitrary polarization reconfiguration. By rapidly modulating the states of the dual-polarization-multiplexed reconfigurable element using carefully designed time series, independent control of the reflected amplitude and phase in both polarization channels can be achieved at both fundamental and harmonic frequencies [23], [24]. Synthesizing the two independent polarizations, it is possible to generate arbitrary polarizations in real time, covering the entire Poincaré sphere.

To address the dual requirements of beam alignment and polarization synchronization in wireless communications, it is essential to develop an antenna that possesses both beam-steering and polarization-reconfigurable capabilities. By using the temporal-modulation technique with carefully designed time series, the beam-pattern reconfiguration and arbitrary polarization switching function is realized [25]. However, this approach suffers from reduced energy efficiency due to modulation at harmonic frequencies, which leads to reduced amplitude at the fundamental frequency. To overcome the efficiency loss, a novel method was proposed in [26], presenting a 1-bit beam-scanning RRA capable of achieving HLP,

This work was supported in part by THE XPLOER PRIZE. (Corresponding author: Fan Yang.)

The authors are with the Beijing National Research Center for Information Science and Technology (BNRist), Department of Electronic Engineering, Tsinghua University, Beijing 100084, China (e-mail: fan_yang@tsinghua.edu.cn).

VLP, LCP and RCP reconfigurations. This method employs a dual-LP-multiplexed 1-bit RRA, whereby the reference phase constants of the two polarization channels are adjusted to synthesize the desired polarization at the target beam direction. However, this design does not allow for the generation of arbitrary LPs.

In this paper, we propose a beam-steering RRA that enables arbitrary LP reconfiguration. By leveraging a dual-CP-multiplexed 1-bit RRA, arbitrary LPs can be synthesized by manipulating the relative phase of the dual-CP directional waves. As a demonstration of concept, a 16×16 dual-CP 1-bit RRA operating at 16.8 GHz is employed to generate scanning beams corresponding to LP(0°), LP(45°), LP(90°) and LP(135°), respectively. For each polarization state, the gains and the beam scanning patterns are measured, demonstrating the precise tuning of beam directions and arbitrary LPs as desired. This paper is organized as follows. Section II proposes the operation principle of arbitrary LP synthesis. Section III shows the experimental demonstration of the proposed method. Finally, the conclusion is drawn in Section IV.

II. OPERATION PRINCIPLE

A. Relations Between the Phase Constant and the Wave Phase

To begin with, we establish a lemma: The phase of the reflected EM wave exhibits a linear relationship with the phase constant of the 1-bit RRA.

Let us consider a reflectarray composed of $M \times N$ elements, which is fed by a near-field horn. The reflection from the (m, n) th element possesses a compensation phase denoted as φ_{mn} and a magnitude represented by E_{mn} . Summing all the reflected waves, the total EM wave at the direction $\vec{k} = (\theta_0, \phi_0)$ can be expressed as

$$E = \sum_{m=1}^M \sum_{n=1}^N E_{mn} e^{-j(\varphi_{fmn} - \varphi_{mn} - \vec{k} \cdot \vec{r}_{mn})}. \quad (1)$$

Here, φ_{fmn} represents the phase delay from the feed to the (m, n) th element, and \vec{r}_{mn} denotes the location of the element. Note that the path loss and the phase delay along the path is ignored.

To achieve maximum gain at \vec{k} direction, the required compensation phase for the (m, n) th element should satisfy

$$\varphi_{mn}^{req} = \varphi_{fmn} - \vec{k} \cdot \vec{r}_{mn} + \Delta\varphi, \quad (2)$$

where $\Delta\varphi$ is defined as the phase constant of the reflectarray [1]. If the reflectarray elements can produce continuous compensation phases, the required phase φ_{mn}^{req} can be obtained, with $\varphi_{mn} = \varphi_{mn}^{req}$. Consequently, the total EM wave is

$$E = e^{j\Delta\varphi} \sum_{m=1}^M \sum_{n=1}^N E_{mn}. \quad (3)$$

The magnitude of the total EM wave is not affected by $\Delta\varphi$. However, the variation in the phase constant results in a linear variation in the phase of the EM wave.

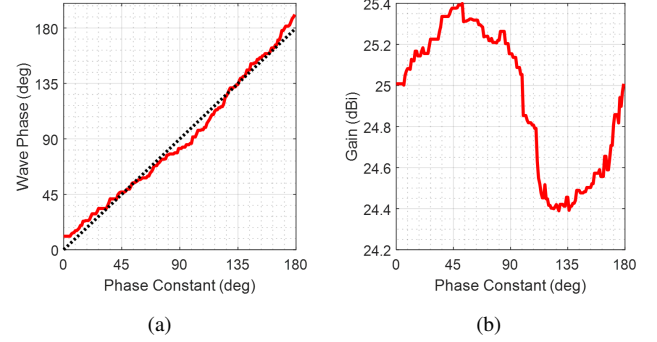


Fig. 1. Simulated reflection wave phases and gains of a 16×16 1-bit RRA. (a) Variation of wave phase with respect to the phase constant. (b) Variation of gain with respect to the phase constant.

For 1-bit RRAs, only two values of φ_{mn} are available. Suppose φ_{mn} can be quantized as 0° or 180° , and the phase quantization strategy is

$$\varphi_{mn} = \begin{cases} 0^\circ & -90^\circ \leq \varphi_{mn}^{req} < 90^\circ \\ 180^\circ & 90^\circ \leq \varphi_{mn}^{req} < 270^\circ \end{cases} \quad (4)$$

We further introduce the phase quantization error

$$\varphi_{mn}^{err} = \varphi_{mn} - \varphi_{mn}^{req}, \quad (5)$$

where $\varphi_{mn}^{err} \in [-90^\circ, 90^\circ]$. Hence, the total EM wave is simplified as

$$E = e^{j\Delta\varphi} \sum_{m=1}^M \sum_{n=1}^N E_{mn} e^{j\varphi_{mn}^{err}}. \quad (6)$$

It has been observed that the distribution of the phase quantization errors is pseudorandom within the range of $[-90^\circ, 90^\circ]$ [27]. According to the law of large numbers, as M and N increase, the phase of $\sum_{m=1}^M \sum_{n=1}^N E_{mn} e^{j\varphi_{mn}^{err}}$ converges towards 0° . Thus, even under the 1-bit phase quantization, the overall phase of the EM wave still exhibits a near-linear variation with the phase constant.

The simulation results based on the 16×16 1-bit RRA provide evidence supporting the theory that the wave phase changes near linearly with the phase constant, as shown in Fig. 1(a). However, due to the pseudorandom property of 1-bit phase quantization, there is a phase error which is within 13° . Furthermore, Fig. 1(b) illustrates the variation in gain with the phase constant, demonstrating a 1-dB range of variation.

In summary, it is found that the phase constant $\Delta\varphi$ serves as a new degree of freedom at the array level to tune the phase of the reflected EM wave from the 1-bit RRA.

B. Arbitrary LP Synthesis Based on Dual-CP RRA

This part highlights the utilization of the phase constant effect to synthesize arbitrary LP waves through adjustment of the relative phase constants associated with LCP and RCP waves.

Suppose there exists a dual-CP 1-bit RRA capable of steering the LCP and RCP beams independently. Since any arbitrary LP is composed of LCP and RCP components with identical amplitudes, when the dual-CP RRA is illuminated

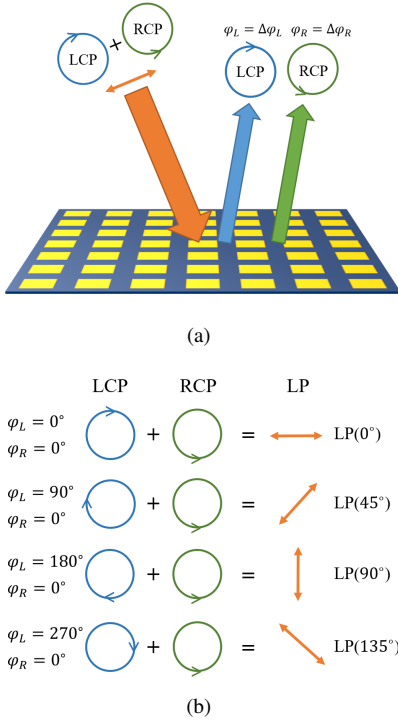


Fig. 2. Schematic illustrations of arbitrary LP generation utilizing the dual-CP RRA. (a) Schematic depicting the generation of dual-CP scanning beams using the LP feed and the dual-CP RRA. (b) Generation of arbitrary LP states by manipulating the relative phases between dual-CP waves.

by an LP feed, it allows for independent manipulation of LCP and RCP beams, as shown in Fig. 2(a). Then, let us examine a scenario in which the LCP and RCP scanning beams are directed towards the same direction. Mathematically, the LCP and RCP waves are represented as

$$E_L = A_L e^{j\varphi_L} \begin{pmatrix} 1 \\ -j \end{pmatrix}, E_R = A_R e^{j\varphi_R} \begin{pmatrix} 1 \\ j \end{pmatrix}. \quad (7)$$

Suppose the amplitudes are equal, denoted as $A_0 = A_L = A_R$. Without loss of generality, let $\varphi_R = 0^\circ$. Combining the two CP waves, the synthesized wave is expressed as

$$E = A_0 \begin{pmatrix} e^{j\varphi_L} + 1 \\ -je^{j\varphi_L} + j \end{pmatrix} = 2A_0 e^{j\varphi_L/2} \begin{pmatrix} \cos(\varphi_L/2) \\ \sin(\varphi_L/2) \end{pmatrix}, \quad (8)$$

which demonstrates that the combination of these two CP waves can generate an LP wave without losing efficiency, and the LP state is determined by φ_L . Geometrically, Fig. 2(b) illustrates the generation of LP(0°), LP(45°), LP(90°) and LP(135°) waves by fixing the phase of the RCP wave and adjusting the phase of the LCP wave.

As discussed in Section II-A, the phase constants of the dual-CP RRA can linearly manipulate the phases of the dual-CP waves. Therefore, by selecting different phase constants, it becomes feasible to generate arbitrary LP states.

An important observation is that arbitrary LPs can only be synthesized using a dual-CP RRA, ensuring no loss in efficiency. As the Poincaré sphere in Fig. 3(a) shows, the equator curve represents all LP states. By manipulating the relative phases of fundamental two CPs, all LP states can be covered. In contrast, Fig. 3(b) portrays the polarization

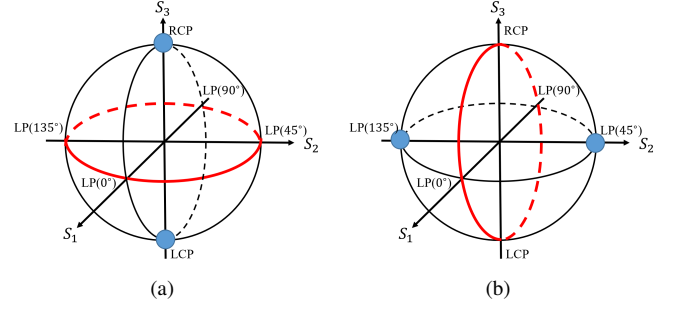


Fig. 3. The Poincaré spheres illustrating the polarization synthesis using the dual-polarized RRAs. The blue dots represent the fundamental polarization states of the RRA, while the red curves represent the synthesized polarizations achievable by adjusting the relative phases between the fundamental polarization states. (a) Schematic demonstrating the synthesis of arbitrary LP states using dual-CP waves. (b) Schematic illustrating the synthesis of LP(0°), LP(90°), LCP, RCP, and EPs using LP(45°) and LP(135°) waves.

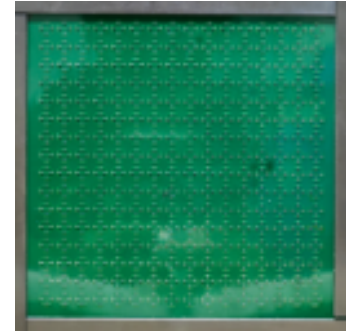


Fig. 4. The 16×16 dual-CP 1-bit RRA prototype.

states that can be synthesized using dual-LP RRAs. These synthesized polarization states from LP(45°) and LP(135°) fundamental waves encompass a meridian, spanning LP(0°), LP(90°), LCP, RCP and elliptical polarizations (EPs). Actually, literature [26] exploits a dual-LP RRA to synthesize the polarization states along a meridian, but it is unable to generate arbitrary LP states on the equator.

III. EXPERIMENTAL DEMONSTRATION

A. Prototype Design

A dual-CP 1-bit RRA element is designed in our previous work, as shown in Fig. 4, with the dimensions labelled in this figure. The period of the element is 8 mm. The top substrate is TLX-8 with a thickness of 1.57 mm, while the bottom substrate is FR-4 with a thickness of 1.4 mm for placing biasing lines, and they are bonded together by a prepreg layer. The reflective ground plane is on the bottom side of the top substrate. Each element integrates four PIN diodes, of which three can be controlled independently. This design allows the element to independently respond to incident waves of LCP and RCP, with the ability to achieve 1-bit phase tuning.

The measured results of the element performance are shown in Fig. 5. The dual-CP 1-bit element offers four distinct states, denoted as State 1, State 2, State 3, and State 4. It operates at a central frequency of 16.8 GHz. For LCP incident and reflected waves, when solely adjusting the LCP states, the reflection

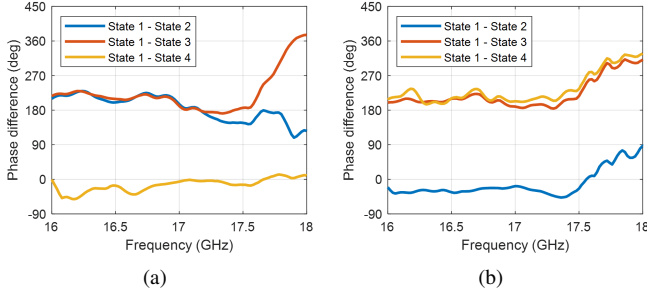


Fig. 5. Measured reflection phase differences for LCP and RCP waves of the element. State 1: LCP-0, RCP-0; State 2: LCP-1, RCP-0; State 3: LCP-1, RCP-1; State 4: LCP-0, RCP-1. (a) Reflection phase differences of LCP wave. (b) Reflection phase differences of RCP wave.

phase differences are consistently close to 180° , whereas only altering the RCP states results in reflection phase differences close to 0° . This behavior is similar for RCP incident waves as well. These results demonstrate that the dual-CP element can independently manipulate the LCP and RCP waves with 180° phase shift, while simultaneously maintaining minimal mutual coupling between the two polarizations.

A 16×16 -element prototype is fabricated, as shown in Fig. 4. To minimize external interference, the prototype is encased in microwave absorbing materials. Literature has effectively demonstrated the independent beam-scanning capabilities for LCP and RCP waves. In this work, we leverage this prototype to show its the beam-scanning ability with the arbitrary LP synthesis function.

B. Verification of the Phase Constant Effect

Firstly, the linear relationship between the wave phase and the phase constant is experimentally verified. The dual-CP RRA is fed by a dual-CP horn under a 30° oblique incident angle. This RRA produces dual-CP pencil-beams directed toward the broadside. A second dual-CP horn, positioned in the far-field of the RRA along the broadside direction, is employed to measure the reflection phases and amplitudes of the 0° beam. When the incident wave is LCP, the reflected wave is also LCP, whereas the incident RCP wave generates an RCP reflected wave. The phase constants are varied from 0° to 180° with a 10° increment for both LCP and RCP cases.

The received amplitudes and phases are measured at 16.8 GHz. Fig. 6(a) and (b) show the relationship between the wave phases and the phase constants for LCP and RCP waves, respectively. The root mean squared errors (RMSEs) between the wave phases and phase constants are found to be 2.4° for the LCP wave and 2.5° for the RCP wave, providing evidence of an excellent linear relationship between the wave phase and phase constants.

The received amplitudes for LCP and RCP waves are also measured, as shown in Fig. 6(c) and (d), respectively. The mean amplitudes for LCP and RCP beams are approximately from -34.5 dB to -34 dB, validating the assumption of equal amplitudes for LCP and RCP. The amplitude variations are within 1.4 dB for LCP and 2.2 dB for RCP, attributed to the pseudorandom nature of 1-bit phase quantization. It is worth

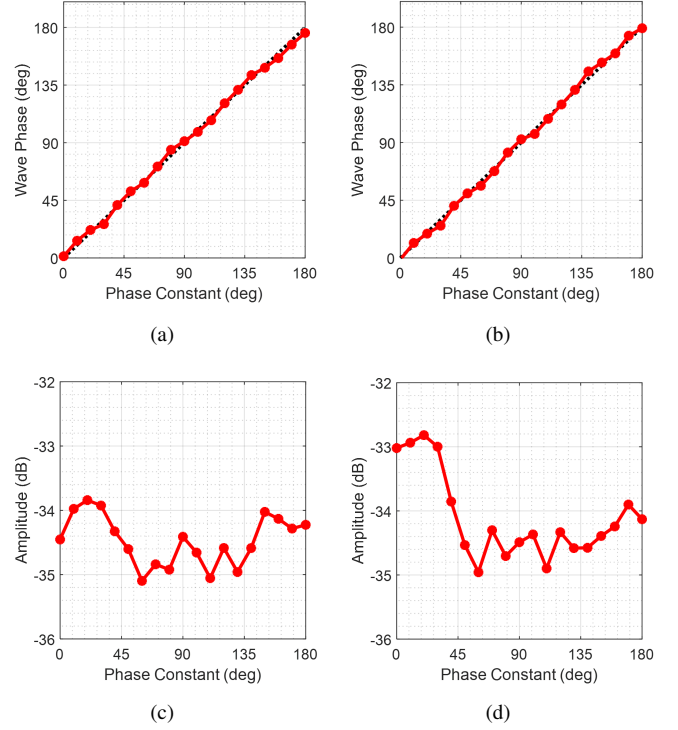


Fig. 6. Measured phases and amplitudes of LCP and RCP waves at 16.8 GHz with varying phase constants. (a) Phase of LCP wave. (b) Phase of RCP wave. (c) Amplitude of LCP wave. (d) Amplitude of RCP wave.

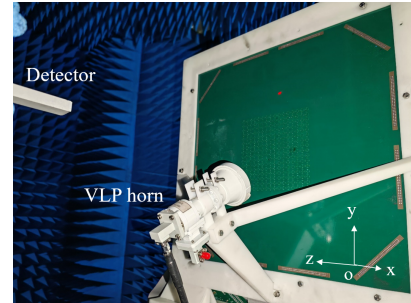


Fig. 7. Measurement setup for polarization-reconfigurable beam steering.

noting that with RRAs possessing higher phase resolution, the amplitude variation range can be reduced.

C. Polarization-Reconfigurable Beamforming Measurement

The beamforming and beam-scanning measurements are conducted in a near-field microwave anechoic chamber. As shown in Fig. 7, the dual-CP RRA is fed by a VLP horn at an oblique incident angle of 30° , with an F/D ratio of 1. The detector moves in xoy plane to measure the field in two orthogonal LPs. To obtain the broadside beam patterns for LPs, both RCP and LCP pencil-beams directed towards 0° . The phase constant for RCP wave is fixed at 0° , while the phase constants for LCP wave varies from 0° , 90° , 135° to 180° , in order to generate LP(90°), LP(45°), LP(22.5°), and LP(0°) beams, respectively.

The measured broadside beam patterns at 16.8 GHz for various LPs are shown in Fig. 8. Clear and well-defined pencil-

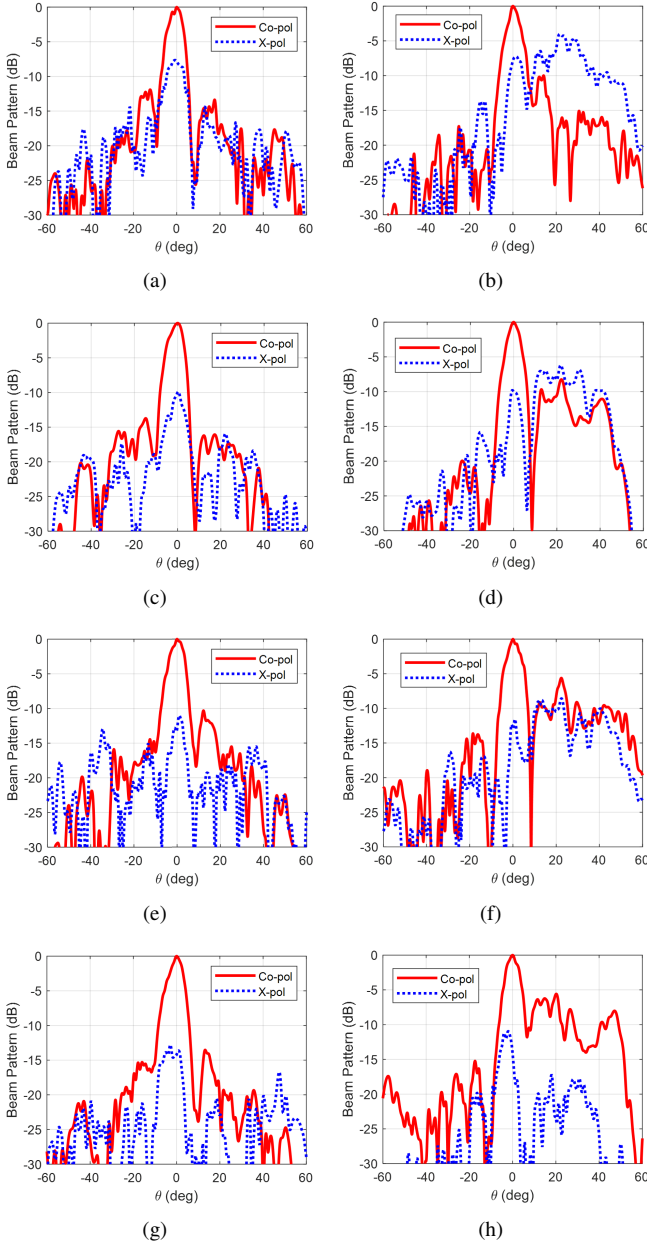


Fig. 8. Measured broadside beams at 16.8 GHz. (a) Broadside beam of LP(0°) in xoz plane. (b) Broadside beam of LP(0°) in yoz plane. (c) Broadside beam of LP(22.5°) in xoz plane. (d) Broadside beam of LP(22.5°) in yoz plane. (e) Broadside beam of LP(45°) in xoz plane. (f) Broadside beam of LP(45°) in yoz plane. (g) Broadside beam of LP(90°) in xoz plane. (h) Broadside beam of LP(90°) in yoz plane.

beams are observed across different polarizations, demonstrating the ability to achieve arbitrary LP configurations as desired. The cross-polarization level remains below -7 dB at a beam angle of 0° for all LPs, indicating acceptable polarization purity. However, in the yoz plane, the sidelobes and cross-polarization levels are relatively high, which is primarily attributed to the specular reflection originating from the feed horn.

The gains of the LP(0°), LP(22.5°), LP(45°) and LP(90°) broadside beams are measured from 16 GHz to 18 GHz, as shown in Fig. 9. It is observed that the gains peak at 16.8 GHz

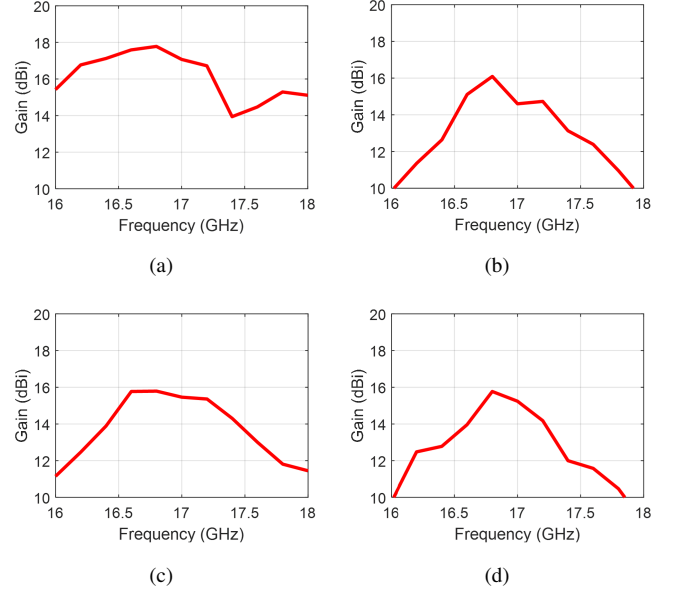


Fig. 9. Measured gains of broadside beams. (a) Gain of LP(0°). (b) Gain of LP(22.5°). (c) Gain of LP(45°). (d) Gain of LP(90°).

for all LP states. At this frequency, the LP(90°) beam achieves a maximum gain of 17.8 dBi, while the LP(0°) beam exhibits the minimum gain of 15.8 dBi. The range of gain variation is 2 dB, primarily influenced by the 1-bit phase quantization. Furthermore, the LP(0°) beam demonstrates a minimum 3-dB gain bandwidth of 5.5%, which aligns with the bandwidth of the dual-CP RRA previously described.

D. Beam Scanning Measurement

The beam scanning patterns for the LP(0°), LP(22.5°), LP(45°), and LP(90°) are measured in both xoz and yoz planes. Fig. 10 illustrates the beam scanning patterns in the xoz plane, showing that all LPs can support scanning up to 60°. Fig. 11 shows the beam scanning pattern in yoz plane. The LP(90°) case demonstrates a scanning range of 60°, albeit with higher sidelobes due to specular reflection from the feed. LP(0°), LP(22.5°), and LP(45°) beams exhibit a scanning range of 30°. In summary, the beam scanning range can support at least 30° in 2-D space.

IV. CONCLUSION

This paper presents a 1-bit RRA that offers both arbitrary LP reconfiguration and beam scanning capabilities. The study first explores the linear relationship between wave phase and phase constant, revealing that the phase constant serves as a novel degree of freedom for manipulating EM wave properties at the array level. Subsequently, LPs are synthesized by employing LCP and RCP directional beams based on the dual-CP RRA. By adjusting the phase constants of the LCP and RCP waves, the arbitrary LP states can be generated and switched as desired. Experimental validations are conducted to verify the proposed method, wherein a dual-CP 1-bit RRA prototype successfully synthesizes reconfigurable LP(0°), LP(45°), LP(90°),

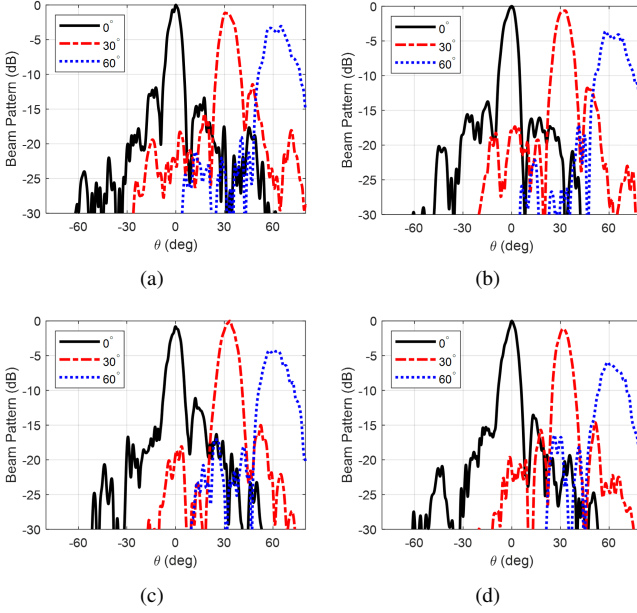


Fig. 10. Measured scanning beams in xoz plane. (a) Scanning beams of LP(0°). (b) Scanning beams of LP(22.5°). (c) Scanning beams of LP(45°). (d) Scanning beams of LP(90°).

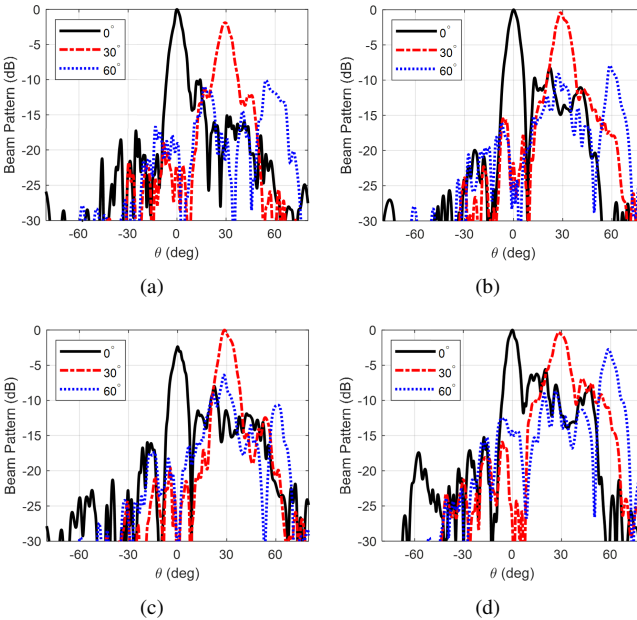


Fig. 11. Measured scanning beams in yoz plane. (a) Scanning beams of LP(0°). (b) Scanning beams of LP(22.5°). (c) Scanning beams of LP(45°). (d) Scanning beams of LP(90°).

and LP(135°) pencil-beams. Furthermore, beam scanning patterns are measured for the four polarization states, revealing a 30° beam scanning range in a 2-D space. The proposed LP-reconfigurable RRA exhibits great potential for applications in wireless communications, particularly in scenarios requiring high-gain beam alignment and polarization synchronization simultaneously.

REFERENCES

- [1] P. Nayeri, F. Yang, and A. Z. Elsherbeni, *Reflectarray Antennas: Theory, Designs and Applications*. New York, NY, USA: Wiley, 2018.
- [2] S. V. Hum and J. Perruisseau-Carrier, "Reconfigurable reflectarrays and array lenses for dynamic antenna beam control: A review," *IEEE Trans. Antennas Propag.*, vol. 62, no. 1, pp. 183–198, Jan. 2014.
- [3] P. Nayeri, F. Yang, and A. Elsherbeni, "Beam scanning reflectarray antennas: A technical overview and state of the art," *IEEE Antennas Propag. Mag.*, vol. 57, no. 4, pp. 32–47, Aug. 2015.
- [4] H. Kamoda, T. Iwasaki, J. Tsumochi, T. Kuki and O. Hashimoto, "60-GHz electronically reconfigurable large reflectarray using single-bit phase shifters," *IEEE Trans. Antennas Propag.*, vol. 59, no. 7, pp. 2524–2531, July 2011.
- [5] H. Yang *et al.*, "A 1-bit 10 × 10 reconfigurable reflectarray antenna: design, optimization, and experiment," *IEEE Trans. Antennas Propag.*, vol. 64, no. 6, pp. 2246–2254, June 2016.
- [6] J. Han, L. Li, G. Liu, Z. Wu and Y. Shi, "A wideband 1 bit 12 × 12 reconfigurable beam-scanning reflectarray: Design fabrication and measurement," *IEEE Antennas Wireless Propag. Lett.*, vol. 18, no. 6, pp. 1268–1272, Jun. 2019.
- [7] H. Zhang, X. Chen, Z. Wang, Y. Ge and J. Pu, "A 1-bit electronically reconfigurable reflectarray antenna in X band," *IEEE Access*, vol. 7, pp. 66567–66575, 2019.
- [8] X. Pan, F. Yang, S. Xu and M. Li, "A 10240-element reconfigurable reflectarray with fast steerable monopulse patterns," *IEEE Trans. Antennas Propag.*, vol. 69, no. 1, pp. 173–181, Jan. 2021.
- [9] B. J. Xiang, X. Dai, and K. M. Luk, "A wideband low-cost reconfigurable reflectarray antenna with 1-bit resolution," *IEEE Trans. Antennas Propag.*, vol. 70, no. 9, pp. 7439–7447, Sept. 2022.
- [10] C. Liu *et al.*, "A radiation viewpoint of reconfigurable reflectarray elements: Performance limit, evaluation criterion and design process," *arXiv preprint arXiv:2211.08632*, 2023.
- [11] B. D. Nguyen, V. S. Tran, L. Mai, P. H. Dinh, "A two-bit reflectarray element using cut-ring patch coupled to delay lines," *REV J. Electronics Communications*, vol. 6, no. 1-2, pp. 30–34, 2016.
- [12] C. Huang *et al.*, "Dynamical beam manipulation based on 2-bit digitally-controlled coding metasurface," *Scientific Reports*, vol. 7, no. 1, pp. 1–8, Feb. 2017.
- [13] X. Yang, S. Xu, F. Yang, and M. Li, "A novel 2-bit reconfigurable reflectarray element for both linear and circular polarizations," in *Proc. IEEE Int. Symp. Antennas Propag. USNC/URSI Nat. Radio Sci. Meeting*, Jul. 2017, pp. 2083–2084.
- [14] S. V. Hum, M. Okoniewski, and R. J. Davies, "Modeling and design of electronically tunable reflectarrays," *IEEE Trans. Antennas Propag.*, vol. 55, no. 8, pp. 2200–2210, Aug. 2007.
- [15] F. Venneri, S. Costanzo, and G. Di Massa, "Design and validation of a reconfigurable single varactor-tuned reflectarray," *IEEE Trans. Antennas Propag.*, vol. 61, no. 2, pp. 635–645, Feb. 2013.
- [16] M. E. Trampler, R. E. Lovato, and X. Gong, "Dual-resonance continuously beam-scanning X-band reflectarray antenna," *IEEE Trans. Antennas Propag.*, vol. 68, no. 8, pp. 6080–6087, Aug. 2020.
- [17] C. Liu, F. Yang, S. Xu, and M. Li, "Reconfigurable metasurface: A systematic categorization and recent advances," *arXiv preprint arXiv:2301.00593*, 2023.
- [18] N. Zhang *et al.*, "A dual-polarized reconfigurable reflectarray antenna based on dual-channel programmable metasurface," *IEEE Trans. Antennas Propag.*, vol. 70, no. 9, pp. 7403–7412, Sept. 2022.
- [19] H. Yang *et al.*, "A programmable metasurface with dynamic polarization, scattering and focusing control," *Sci. Rep.*, vol. 6, no. 35692, pp. 1–11, Oct. 2016.
- [20] H. Yu *et al.*, "Design of a wideband and reconfigurable polarization converter using a manipulable metasurface," *Opt. Mater. Exp.*, vol. 8, no. 11, pp. 3373–3381, 2018.
- [21] X. Ma *et al.*, "An active metamaterial for polarization manipulating," *Adv. Opt. Mater.*, vol. 2, no. 10, pp. 945–949, Oct. 2014.

- [22] J. Cui *et al.*, “Dynamical manipulation of electromagnetic polarization using anisotropic meta-mirror,” *Sci. Rep.*, vol. 6, p. 30771, Jul. 2016.
- [23] Q. Hu *et al.*, “Arbitrary and dynamic Poincaré sphere polarization converter with a time-varying metasurface,” *Adv. Opt. Mater.*, vol. 10, no. 4, Feb. 2022.
- [24] Q. Hu *et al.*, “On-demand dynamic polarization meta-transformer,” *Laser Photonics. Rev.*, vol. 17, no. 1, Jan. 2023.
- [25] Q. Hu *et al.*, “Dynamically generating diverse multi-beams with on-demand polarizations through space-time coding metasurface,” *Adv. Opt. Mater.*, 2300093, 2023.
- [26] J. Hu, P. -L. Chi and T. Yang, “Novel 1-bit beam-scanning reflectarray with switchable linear, left-handed, or right-handed circular polarization,” *IEEE Trans. Antennas Propag.*, vol. 71, no. 2, pp. 1548-1556, Feb. 2023.
- [27] H. Yang *et al.*, “A study of phase quantization effects for reconfigurable reflectarray antennas,” *IEEE Antennas Wireless Propag. Lett.*, vol. 16, no. 5, pp. 302-305, Mar. 2017.